JOURNAL OF MATERIALS SCIENCE 32 (1997) 6235–6242

Residual stress measurements of computer aided design/computer aided manufacturing (CAD/CAM) machined dental ceramics

F. GRELLNER, S. HÖSCHELER, P. GREIL
Department of Materials Science, Glass and Ceramics, University Erlangen-Nuremberg, Martensstrasse 5, 91058 Erlangen, Germany

J. SINDEL, A. PETSCHELT
Policlinic of Operative Dentistry and Periodontology, University Erlangen-Nuremberg, Glückstrasse 11, 91054 Erlangen, Germany

Residual stress analysis is becoming more important in terms of understanding the strength and fatigue behaviour of ceramic materials. The residual stresses after computer aided design/computer aided manufacturing (CAD/CAM) machining according to dental practice were analysed for two different kinds of dental ceramics, a feldspathic porcelain and a glass–ceramic. A mechanical strain gauge element was used to measure the deformation of dental test inlays during material removal by etching the surface of the sample. From these data the residual stress depth profile could be calculated for crystalline as well as amorphous materials. The strain gauge results were compared to X-ray diffraction data. The depth profile of the residual stress for both ceramics showed compressive stress at the surface of the machined ceramics, changing towards tensile stress at a depth of 10 to 15 μm from the surface. Ceramics with pronounced plastic deformation behaviour in CAD/CAM machining revealed higher residual stresses as well as a more distinct stress anisotropy in terms of grinding direction.

1. Introduction

Due to the increasing aesthetic demands of patients together with a rising concern about the biocompatibility of dental amalgam for tooth restorations, ceramic dental materials are becoming more important in dentistry. Basically, the fabrication of ceramic inlays can be divided into two routes [1]. A conventional tooth laboratory prepares the inlay using a lost-wax process and slip-casting, controlled crystallization of glass or hot-pressing of precrystallized glasses. This is a time-consuming procedure and the quality of the inlay depends on the skill of the technician. In addition, process dependent microdefects reduce the fracture strength and increase the time-dependent failure probability of these restorations [2].

Efforts to automate the production of dental restorations have initiated the development of computer aided design/computer aided manufacture (CAD/CAM) units to process dental ceramics starting from prefabricated ceramic blocks (called preforms). These preforms are manufactured under controlled conditions resulting in a ceramic material with only small variations in microstructure. The ceramic blocks can be machined with diamond grinding wheels, according to the scanning data of the cavity using a small charge coupled device (CCD) camera inside the mouth of the patient [3]. The inlay can be manufactured in one appointment, the so called chairside-concept.

Machining of materials induces residual stresses. This is well-known for metals, where the formation of these stresses and their impact on component behaviour have been evaluated extensively [4–9]. In the field of ceramics and glasses, residual stresses are commonly used to increase the fracture strength of components, but detailed information about manufacturing related residual stresses is scarce [10]. In recent years, this gap has begun to be closed [11–16]. For brittle materials, surface residual stresses can have an enormous effect on the fracture behaviour. It should be pointed out that compressive residual stresses caused by tempering of glass or ion exchange can increase flexural strength by a factor of five [17].

In this paper, the residual stress profiles caused by CAD/CAM machining of dental ceramics will be evaluated using two different stress measurement techniques: X-ray diffraction and mechanical strain gauge measurements. Even though grinding is a common procedure to machine dental ceramics, no information has been published about the generation of residual stress during machining. This is surprising, as the resulting strength of a part is governed by externally applied loading stresses as well as by internal residual stresses [18]. Consequently, the evaluation of residual stress levels is of considerable significance for the understanding of properties and performance of mechanically machined dental restorations.

0022–2461

1.1. Residual stresses

Residual stresses are self-equilibrating stresses, that exist in materials under uniform temperature conditions without external loading. Therefore, the resulting forces and moments are in mechanical equilibrium and neutralize each other over the volume of the whole part.

Residual stresses result from inhomogeneous elastic or plastic deformations in such a permanent manner that incompatibilities in the state of deformation occur [19]. These deformations can be induced thermally, mechanically or via phase transformations. From a technological point of view, manufacturing, processing or joining of materials will always induce some kind of irreversible deformation [20–23]. Thus, in reality, no technical part is free of residual stresses.

A standardized system of designation classifies three different kinds, called residual stresses of 1st, 2nd and 3rd kind [19, 20]. The 1st kind of residual stresses are homogeneously distributed across large areas of a material and are representing the mean stress level. These kind of residual stresses are also called macro residual stresses. A change in the equilibrium of such a stress state will always result in a macroscopic change in dimension. Residual stresses of the 2nd kind are uniform across microscopic areas (i.e., one grain or parts of a grain). They are also called homogeneous micro residual stresses. A change in the equilibrium of this kind of residual stress can result in dimensional changes, too. Residual stresses of the 3rd kind are inhomogeneous, even across submicroscopic areas. Vacancies, dislocations and impurity atoms typically cause this kind of residual stress state. A change in the equilibrium of such a stress will not result in a macroscopic change in dimension.

The total residual stress state at a distinct point of the material can be expressed by the superposition of all three kinds of residual stresses. Depending on the type of measurement, different kinds of residual stresses can be detected, as summarized in Table I.

Although the term stress measurement has come into common usage, stress is an extrinsic property that is not directly measurable. Therefore, all methods of stress determination require measurements of some intrinsic property such as strain, force or shape in combination with a calculation of the associated stress [27]. X-ray diffraction and mechanical strain gauge procedures are most commonly used for the evaluation of residual stress and these two methods will be applied in this study. Throughout this paper, by definition, compressive residual stresses will have a negative sign and tensile residual stresses a positive sign.

2. Experimental procedure

Two commercially available dental ceramics were investigated; (i) Vitablocs Mark II® (Vita Zahnfabrik, Bad Säckingen, Germany) and (ii) Dicor MGC® (Dentsply, Milford, USA). Both materials were supplied from the manufacturer as a preform for CEREC® machining.

Vitablocks Mark II® is a fine particle feldspathic porcelain situated in the quarternary system K_2O–Na_2O–Al_2O_3–SiO_2. The percentage of potash feldspar in the raw material is about 80 wt %. The raw materials mixture is milled and extrusion moulded to yield the CEREC® preform. In the sintered product, the glassy phase content is about 80 vol %. Fig. 1 shows the microstructure of an etched Vitablocs sample. The glassy phase dominates the microstructure, but small crystallites of mixed nepheline (Na, K[$AlSiO_4$]), albite (Na[$AlSi_3O_8$]) and orthoclase (K[$AlSi_3O_8$]) with a mean size of 2–5 μm can be observed.

Dicor MGC® is a tetrasilicic fluormica glass–ceramic containing K_2O, SiO_2, MgO, Al_2O_3, B_2O_3 and MgF_2 [28]. In contrast to the feldspathic porcelain, the crystalline content dominates the microstructure of the glass–ceramic (70 vol %). The preform is manufactured by casting and subsequent controlled crystallization. The microstructure of an etched Dicor sample can be seen in Fig. 2, showing plate-like

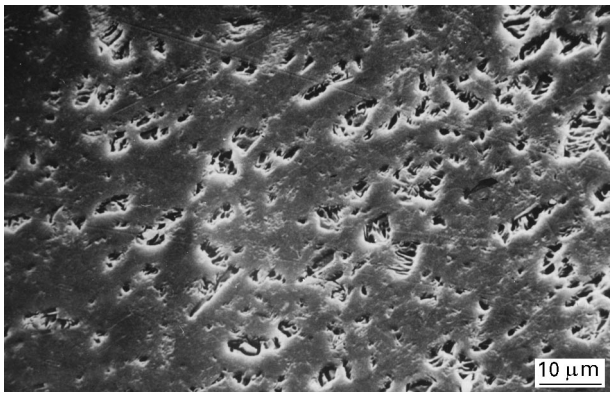

Figure 1 SEM micrograph of the microstructure of the Vitablocs Mark II® ceramic (etched 1 min, 5% HF).

TABLE I Residual stress measurements and their characteristics after [25, 26]

Type of measurement	Measured quantities	Residual stresses determined 1st 2nd 3rd kind	Character
Mechanical	Macroscopic strains	×	Destructive
X-ray diffraction	Homogeneous lattice strains (at the surface)		Non-destructive
Line Shift		× ×	
Line Broadening		× ×	
Neutron diffraction	Homogeneous lattice strains	× ×	Non-destructive
Magnetic		× × ×	Non-destructive
Ultrasonic		× × ×	Non-destructive

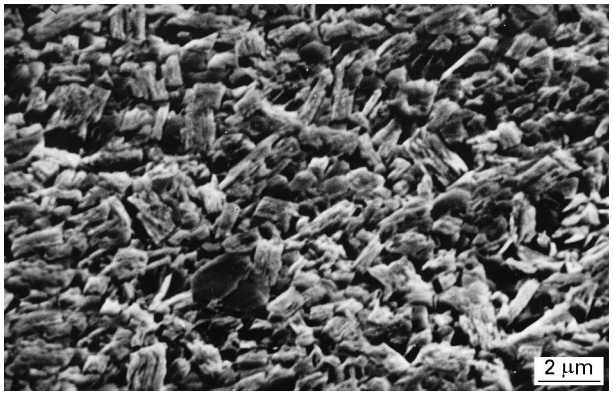

Figure 2 SEM micrograph of the microstructure of the Dicor MGC® glass–ceramic (etched 1 min, 5% HF).

fluormica crystals ($KMg_{2.5}Si_4O_{10}F_2$) with a mean size of 1–2 μm. The properties of these two ceramics are summarized in Table II.

The ceramic preforms were machined with a CEREC 1® system (Siemens AG, Bensheim, Germany), a dental CAD/CAM machining device with a high speed diamond grinding wheel. The average grain size of the diamond particles was 64 μm and the unloaded surface speed of the grinding disc was 45 m s^{-1}. During operation, the surface speed of the disc is reduced to 21 m s^{-1}. Surface tension was reduced by adding a combined detergent and lubricant (CEREC® Dentagrind 2000, Siemens AG, Bensheim, Germany) to the cooling water. The samples were machined to the shape of a computer generated rectangular test inlay ($10 \times 10 \times 0.4$ mm) according to dental practice. The geometric arrangement of sample and grinding disc is shown in Fig. 3.

Measurement of the temperature increase on the surface during the CEREC® machining were performed with thermocolours (Thermal indicating paint, Thermographics Measurements, MA, USA) on the upper surface of the ceramic specimen following the techniques of Vieregge [29]. Machining was stopped when the contact zone between the thermocolour and the ceramic was exposed. The temperature generated on the surface of the specimen could be estimated by comparison with standard calibration samples.

The surface morphology was examined by scanning electron microscopy (SEM) using a Leitz microscope (Leitz-ISI SR 50®, Akashi Corp., Japan). To evaluate the microstructure of the ceramics (see Figs 1 and 2), the samples were etched for 60 s using Vita CEREC®-etch (5% HF).

The residual stress measurements using X-rays (method 1) were performed using a Siemens D 5000 diffractometer, equipped with an open Eulerian cradle and a position sensitive detector. The analysis was performed with Cr-K_α radiation (wavelength $\lambda = 0.2291$ nm) according to the widely used $\sin^2\psi$-method [30–32]. For the Dicor ceramics, the (211) diffraction peak of fluormica at $2\theta = 122.4^\circ$ was chosen, whereas for the Vitablocs no suitable diffraction peak could be found because of the high amount of glassy phase. The calculation of the residual stress values was performed on a personal computer using the "Stress AT" software (Socabim, Siemens AG, Germany) and the material constants listed in Table II. More details about this procedure can be found in the appendix and in the literature [33].

Residual stress measurements were also performed using a mechanical strain gauge procedure (method 2). This method is based on the continuous measurement of changes in shape due to removal of stressed material layers on one side by an etching treatment. A strain gauge element (LY 61 1.5/120, HBM, Darmstadt, Germany) was used for the detection of the curvature of the sample by amplifying and recording the changes in resistance versus the etching time with a scanning rate of 1 Hz. A second sample, covered with an etch-resistant coating, was used for compensating the temperature drift during the measurement. Fig. 4 is a schematic illustration of the experimental setup.

The etching rate of the ceramics using 10% HF was calibrated independently to be 5 μm min^{-1} for the Dicor MGC® and 10 μm min^{-1} for the Vitablocs,

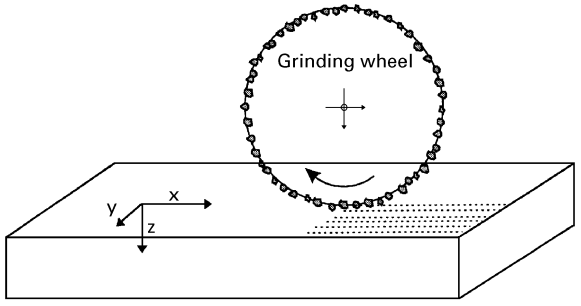

Figure 3 Geometric arrangement of sample and grinding wheel.

TABLE II Properties of the Vitablocs and Dicor dental ceramics

	Vitablocs Mark II®	Dicor MGC®
Major components	SiO_2 K_2O, Na_2O, Al_2O_3,	SiO_2, K_2O, MgO, MgF_2
Crystalline phase content (vol %)	20	70
Major crystalline phases	Orthoclase ($KAlSi_3O_8$) Albite ($NaAlSi_3O_8$)	Fluormica ($KMg_{2.5}Si_4O_{10}F_2$)
Young's modulus E (GPa)	63	70
Poisson's ratio ν	0.23	0.23
Density ρ (g cm^{-3})	2.5	2.8
Coefficient of thermal expansion α (K^{-1})	8.0×10^{-6}	6.5×10^{-6}

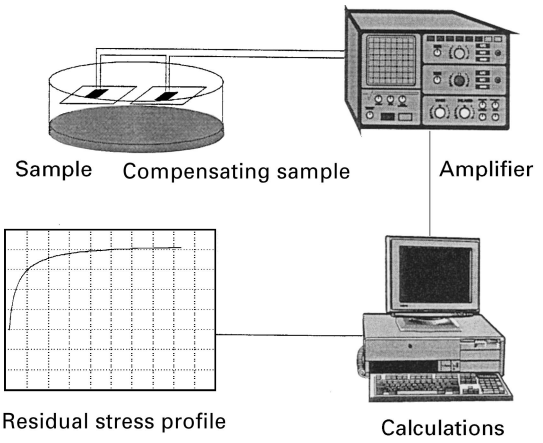

Figure 4 Experimental setup for the detection of residual stresses by a strain gauge measurement.

respectively. From these data, the profile of residual stress versus depth of removal can be calculated using the material constants listed in Table II as well as numerically solving Equations A5 and A6, as described in the appendix.

3. Results and discussion

3.1. Temperature increase during CAD/CAM machining

During the machining of ceramics, a temperature increase at the surface of the material can occur. The mechanism of heat generation in the contact zone between the grinding wheel and ceramic is not fully understood [14]. In the machining of metals, temperatures in the range of 300–500 °C can be calculated from adiabatic approximations [29].

During the machining of both the Vitablocs and Dicor ceramics no change in colour occurs, indicating that the onset temperature of the thermocolour (300 °C) has not been reached. This is a clear evidence that thermally activated processes such as viscous flow, creep or grain boundary slip should be of minor importance.

3.2. X-ray diffraction

Residual stress measurements using X-ray diffraction could only be performed on the Dicor MGC® ceramics because of the low crystallinity of the Vitablocs Mark II®. The data were collected from 4 independent measurements. The residual stress analysis showed compressive stresses $\sigma_x = -30 \pm 8$ MPa in the grinding direction and $\sigma_y = -49 \pm 20$ MPa in the transverse direction. The lower values for the residual stress observed parallel to the machining grooves are in agreement with the results obtained by other authors [34–36]. These results show a few limitations, however: (i) Dicor MGC® is a two-phase material containing both a crystalline and an amorphous phase. Residual stresses of multi-phase materials can only be measured exactly by independent evaluation of the lattice strain for each phase [37]. Since the glassy phase is amorphous, the measured stress values only represent the crystalline fluormica phase. (ii) Machined ceramic materials typically show steep gradients in residual stress perpendicular to the surface [34, 38, 39]. The evaluation of the X-ray measurements using the $\sin^2\psi$-method is based on a linear dependence between the lattice strains and $\sin^2\psi$. However for large gradients this linear dependence may change to a parabolic one [35, 40]. (iii) A third source of error is the anisotropy of the mica crystals. Most of the residual stress measurements were performed on materials with a high symmetric crystallographic order (i.e., metals). There is only limited knowledge on residual stress measurements of anisotropic materials such as fluormica, a sheet silicate. Perhaps, this error could be compensated for by direct determination of the Voigt's constants [35]. (iv) The results from these measurements only represent the weighted mean value of the residual stresses according to the penetration depth of the X-rays (see appendix for details) and does not give any information about the depth profile.

3.3. Strain gauge measurements

Because of these limitations, a second method for the determination of the residual stress was used where both materials, the almost amorphous feldspathic porcelain as well as the glass–ceramic, could be analysed. This method is based on the continuous measurement of changes in shape due to the removal of stressed material layers by an etching treatment. All depth profiles represent the mean of 5 independent measurements. Figs 5 and 6 show the residual stress profiles of the machined Vitablocs Mark II® and Dicor MGC® ceramics, respectively. The compressive nature of residual stress in the outer layer of the machined ceramics, as determined via X-ray diffraction, is confirmed. Each of the two dental ceramics shows a different behaviour in CAD/CAM machining, according to their microstructure. Due to the high amount of glassy phase (see Fig. 1), the feldspathic porcelain (Vitablocs Mark II®) shows microcracking and extensive chipping. The microcracks can extend up to 50 μm from the surface [41]. Therefore, plastic deformation is minor and consequently, the residual stress values for

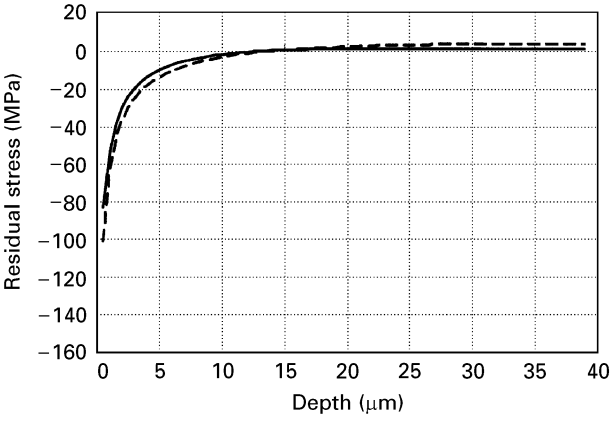

Figure 5 Residual stress profile of a machined Vitablocs Mark II® ceramic in the grinding direction (——) and perpendicular (– – – – – –) to the grinding direction.

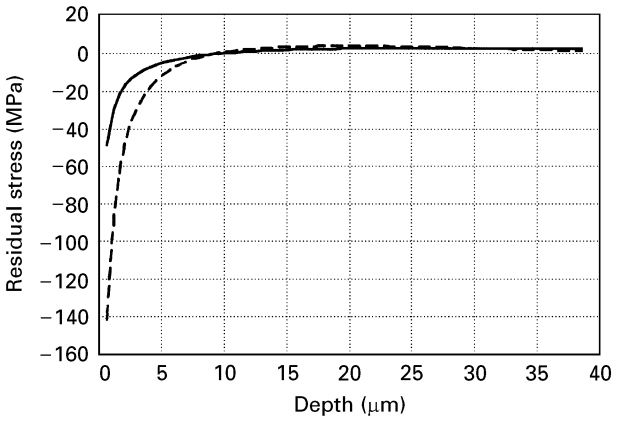

Figure 6 Residual stress profile of a machined Dicor MGC ceramic in the grinding (——) direction and perpendicular (– – – – –) to the grinding direction.

the machined ceramic are relatively low. The compressive stresses in the outer layer of the machined ceramic reach a value of $\sigma_x = -85$ MPa in the grinding direction and $\sigma_y = -102$ MPa perpendicular to the grinding direction. The compressive stress decreases and is changing towards tensile stress at a distance of 15 μm from the surface. No X-ray diffraction data are available for comparison.

Even though the compressive residual stresses can reach −100 MPa, the strength of the feldspathic porcelain is determined by surface cracks. These surface cracks extend over the compressed regime of the surface layer (40–50 μm crack extension in comparison to the 15 μm extension of the compressed zone). Therefore, removal of the surface layer by lapping increases the fracture strength [41, 42].

Dicor MGC®, a machinable glass–ceramic, is a sheet silicate of the fluorine–mica family. The microstructure is composed of interlocked plate-like mica crystals (see Fig. 2) which can be easily delaminated along their cleavage planes. Therefore, cracks prefer to solely propagate along these planes. The random intersection of these crystals in the glass–ceramic causes all kinds of energy dissipating processes such as crack branching, deflection, and blunting. These fracture arresting mechanisms enable the glass–ceramic to be readily machined without extended microcracking or chipping [43, 44]. This is confirmed by scanning electron micrographs of machined Dicor ceramics, which show only small surface damage in a μm scale compared to Vitablocs [41]. The dominating process in machining this glass–ceramic is crushing and crumbling with a major contribution of plastic deformation in a microscopic scale [45]. This is a typical behaviour for a ceramic with a small grain size and a high fracture toughness [10].

Due to a higher degree of plastic deformation compared to the feldspathic porcelain, higher but more anisotropic compressive residual stresses ranging from $\sigma_x = -48$ MPa parallel to $\sigma_y = -140$ MPa perpendicular to the machining grooves (see Fig. 6) were detected. This is in agreement with recent investigations that have reported a higher degree of residual stress generation for ceramics that show plastic deformation behaviour in response to grinding machining [46].

The change from compressive to tensile stress occurs at a distance of 10 μm from the surface. It can be concluded that the consequences of the grinding process for the subsurface region is much more pronounced for the Vitablocs than for the Dicor MGC® ceramics, both in terms of crack extension [41] and extension of residual stresses. The surface cracks extend almost into the region of compressive stresses. Therefore, removal of the surface layer does not change the strength of the machined sample significantly. Sealing of these surface cracks, however, increases the fracture strength of machined Dicor ceramics by 40% [41, 42].

Residual stress values in the grinding direction are generally lower than those measured in the transverse direction [34–36]. This can be explained by the fact that the machining impact, resulting in plastic deformation of the ceramic, is extending mainly perpendicular to the grinding grooves. This anisotropy in the residual stress is much less pronounced for the Vitablocs Mark II® than for the Dicor MGC® ceramic. The diffuse microcracking of the feldspathic porcelain does not induce any strong directional dependency to the machined sample. This is confirmed by the fact that no grinding furrows can be observed after the machining of the Vitablocs Mark II® ceramic [41].

3.4. Comparison of X-ray diffraction and strain gauge measurements

The residual stress profile from the strain gauge measurements on the Dicor ceramics was combined with the calculated penetration depth of the X-rays in order to compare these two types of stress analysis (see appendix). Using mass-absorption coefficients for Cr-K_α radiation obtained from the literature [47–48] and interpolating these data for phlogopite ($KMg_3AlSi_3O_{10}F_2$), the mean penetration depth (defined as the thickness of the surface layer which contributes to 63% of the diffracted intensity) can be estimated to be $\bar{z} = 10$ μm. A numerical approach, where the residual stress profile of the strain gauge measurement is weighted by the remaining X-ray intensity, yields a mean value of $\sigma_y = -21 \pm 7$ MPa for the residual stress; a figure which is directly comparable to the value of $\sigma_y = -49 \pm 20$ MPa from the X-ray diffraction measurement. This calculation can

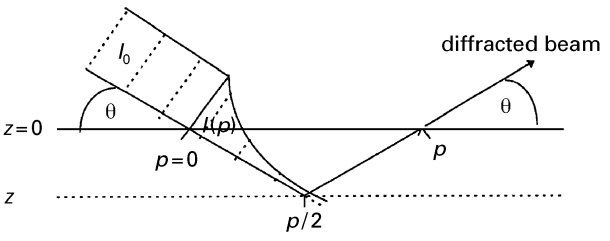

Figure 7 Intensity loss of monochromatic X-rays diffracted at a depth z of a material.

only be taken as a rough estimation to compare these two methods, but it can be concluded that the strain gauge procedure results in smaller residual stress values compared to the X-ray diffraction method. Differences up to a factor of two for the determination of residual stress profiles using different measurement techniques is not uncommon [49].

4. Conclusion

Residual stress analysis is important if an understanding of the strength and fatigue behaviour of ceramic dental materials is to be obtained. X-ray diffraction is a commonly used method, but it can only be applied to materials containing a significant content of crystalline phases. Therefore, an alternative method was additionally applied, namely using a strain gauge to measure the deformation of a sample during etching to remove the stressed surface. The strain gauge data were compared to the data obtained by X-ray diffraction.

The depth profile of the residual stresses for both ceramics could be evaluated, showing compressive stress in the outer layer of the ceramic. The microstructure of the ceramic dominates the machining behaviour as well as the generation of a residual stresses. Ceramics which exhibit plastic deformation behaviour, show higher residual stress levels as well as more pronounced stress anisotropy compared to brittle ceramics after CAD/CAM machining, respectively. For the glass–ceramic, both surface cracks and residual stress contribute to the strength properties of machined samples.

Due to the high amount of glassy phase, the brittle feldspathic porcelain shows extended chipping and microcracking. The compressive stress in the outer layer is more isotropic, compared to the glass–ceramic, but lower in absolute value. Even though the compressive residual stress can reach 100 MPa for the feldspathic porcelain, the strength is dominated by surface cracks. This can be explained by the correlation between the residual stress profile and the extension of microcracks caused by CAD/CAM machining.

Appendix

X-ray diffraction

The fundamental equation for the residual stress analysis using X-rays can be written as [18, 21–23]:

$$\begin{aligned}\varepsilon_{\varphi\psi} &= -\tfrac{1}{2}\cot\theta_0(2\theta_{\varphi\psi} - 2\theta_0)\\ &= \tfrac{1}{2}s_y[\sigma_{xx}\cos^2\varphi + \sigma_{xy}\sin(2\varphi) + \sigma_{yy}\sin^2\varphi - \sigma_{zz}]\\ &\quad \sin^2\psi + \tfrac{1}{2}s_y[\sigma_{xz}\cos\varphi + \sigma_{yz}\sin\varphi]\sin(2\psi)\\ &\quad + (\tfrac{1}{2}s_y + s_x)\sigma_{zz} + s_x[\sigma_{xx} + \sigma_{yy}] \qquad \text{(A1)}\end{aligned}$$

where $\varepsilon_{\varphi\psi}$ is the lattice strain determined in azimuth φ and distance angle ψ; θ_0 is the diffraction angle of the unstrained sample; θ is the diffraction angle of the strained sample; σ_{xy} is the residual stress tensor in the direction $(0, 0)$ to (x, y) and s is Voigt's constant ($\frac{1}{2}s_y = (1 + \nu)/E$ and $s_x = -\nu/E$) where ν is the Poisson's ratio and E is the Young's modulus. The assumption of a biaxial residual stress, parallel to the surface, can be stated to be valid for the surface layer, accessible via X-ray diffraction. Assuming $\sigma_{zz} = 0$, it can be written that:

$$\varepsilon_{\varphi\psi} = \tfrac{1}{2}s_y\sigma_\varphi\sin^2\psi + s_x(\sigma_{xx} + \sigma_{yy}) \qquad \text{(A2)}$$

and

$$\sigma_\varphi = \sigma_{xx}\cos^2\varphi + \sigma_{xy}\sin(2\varphi) + \sigma_{yy}\sin^2\varphi \qquad \text{(A3)}$$

From Equation A2, the lattice strain $\varepsilon_{\varphi\psi}$ (or equivalent $2\theta_{\varphi\psi}$) can be measured in different directions ψ and plotted versus $\sin^2\psi$. From the slope of the linear fit, the integral residual stress value σ_φ can be calculated as:

$$\sigma_\varphi = \frac{2\partial\varepsilon_{\varphi\psi}/\partial(\sin^2\psi)}{s_y} \qquad \text{(A4)}$$

Strain gauge measurements

The residual stress profile can be derived from the strain gauge measurement by calculating the mechano-elastic fundamentals. Using Hook's law, the biaxial residual stresses σ_x and σ_y can be written as [24]:

$$\sigma_x(z) = \frac{E}{1-\nu^2}\left[z^2\frac{d}{dz}(P_x + \nu P_y) + 4z(P_x + \nu P_y) - 2\int_z^{z_o}(P_x + \nu P_y)\,dz\right] \qquad \text{(A5)}$$

$$\sigma_y(z) = \frac{E}{1-\nu^2}\left[z^2\frac{d}{dz}(P_y + \nu P_x) + 4z(P_y + \nu P_x) - 2\int_z^{z_o}(P_y + \nu P_x)\,dz\right] \qquad \text{(A6)}$$

where: $\sigma_{x,y}(z)$ are the residual stresses in the x or y directions at a depth z; z is the actual thickness of the inlay in the course of the etching process; z_0 is the starting thickness of the inlay and $P_{x,y}$ is the curvature in the x or y direction.

These equations are uncertain for the starting thickness z_0, but can be solved for infinitesimally small increments of z using numerical procedures [12]. Therefore, a residual stress profile can be calculated from the strain gauge data, where $\sigma(z)$ represents the residual stress at a depth z of the machined test inlay.

Comparison between X-ray and strain gauge data

The penetration depth of the X-rays into the Dicor ceramics can be estimated from:

$$dI = -\mu I(p)\,dp \qquad \text{(A7)}$$

where μ is the linear absorption coefficient and $I(p)$ the intensity at a distance p. The loss of intensity dI compared to the initial intensity I_0 is due to absorption, scattering, and diffraction (see i.e., [50]). In this paper, the linear absorption coefficient of phlogopite

($KMg_3AlSi_3O_{10}F_2$) is calculated for Cr-K_α radiation according to:

$$\frac{\mu}{\rho} = \sum_i c_i K_i \tag{A8}$$

where K_i is the mass-absorption coefficient of the ith element [47–48]. Integration of Equation A7 yields:

$$I(p) = I_0 \exp(-\mu p) \tag{A9}$$

Equation A9 can be written as a function of the distance from the surface z:

$$I(z) = I_0 \exp(-\mu z/z^*) \tag{A10}$$

where z^* is the penetration depth for which $I(z^*) = (I_0/e)$. z^* is determined by the geometric arrangement of the diffractometer and is dependent on ψ and θ. For a ψ-diffractometer, the relation between the distance from the surface z and the distance travelled by the X-rays, p, can be expressed as:

$$z = \frac{p}{2} \sin\theta \cos\psi \tag{A11}$$

Therefore, the penetration depth can be calculated from Equations A9 and A10

$$z_\psi^* = \frac{\sin\theta \cos\psi}{2\mu} \tag{A12}$$

In this measurement, the minimum distance angle of ψ was 10°, the maximum angle 60°. Therefore, both a minimum and maximum penetration depth z_{min} and z_{max} could be calculated. The mean penetration depth is $\bar{z} = (z_{min} + z_{max})/2$.

To calculate a mean residual stress value $\sigma_y(\bar{z})$, the residual stress profile from the strain gauge measurement is expressed by a numerical function and added as $\sigma_{y(z)}$ to the following equation [21–23, 36]:

$$\sigma_y(\bar{z}) = \frac{1}{\bar{z}} \int_0^\infty \sigma_y(z) \exp\left(-\frac{z}{\bar{z}}\right) dz \tag{A13}$$

Using the residual stress profile $\sigma_{y(z)}$ from the strain gauge data, $\sigma_y(\bar{z})$ can be calculated that represents the expected residual stress value that would have been measured by X-ray diffraction.

References

1. G. SCHMALZ, M. FEDERLIN and W. GEURTSEN, *Dtsch. Zahnaerztl. Zeitschr.* **49** (1994) 197, (in German).
2. J. W. McLEAN, *Operative Dentistry* **16** (1991) 149.
3. W. MÖRMANN and M. BRANDESTINI, "The Cerec Computer Reconstruction," (Quintessenz Verlag, Berlin, 1989) (in German).
4. H. H. LESTER and R. H. ABORN, *Army Ordinance* **6** (1925/26) 120.
5. *Idem*, *ibid* **6** (1925/26) 200.
6. *Idem*, *ibid* **6** (1925/26) 283.
7. *Idem*, *ibid* **6** (1925/26) 364.
8. T. SHIRAIWA and Y. SAKAMOTO, *J. Soc. Mater. Sci.* Jpn. **16** (1967) 343.
9. V. HAUK, W. K. KRUG, R. W. M. OUDELHOVEN and L. PINTSCHOVIUS, *Z. Metallkde* **79** (1988) 159.
10. G. SPUR, "Ceramic Machining," (Carl Hanser Verlag, München, 1989), (in German).
11. F. F. LANG, M. R. JAM and D. J. GREEN, *J. Amer. Ceram. Soc.* **2** (1983) C16.
12. I. BURESCH, PhD thesis, MPI Stuttgart, (1989), (in German).
13. J. C. CONWAY and J. J. MECHOLSKY, *J. Amer. Ceram. Soc.* **72** (1989) 1584.
14. H. G. WOBKER, "Grinding of Ceramic Cutting-tools," (VDI-Verlag, Düsseldorf, 1992), (in German).
15. K. ASAOKA, N. KUWAYAMA and J. A. TESK, *J. Dent. Res.* **71** (1992) 1623.
16. B. EIGENMANN and E. MACHERAUCH, *Z. Metallkde* **86** (1995) 84.
17. R. A. McMASTER, D. M. SHETTERLY and A. G. BUENO, in "Ceramics and Glasses," (ASM International, Materials Park, OH, 1991) p. 453.
18. H. D. TIETZ, "Fundamentals of Residual Stresses," (VEB Deutscher Verlag für Grundstoffindustrie, Leipzig, 1983), (in German).
19. V. HAUK, P. HÖLLER and E. MACHERAUCH, in Proceedings of the International Conference on Residual Stresses, Vol. 1, Garmisch Partenkirchen (FRG), 1986, edited by E. Macherauch and V. Hauk, (Deutsche Gesellschaft für Metallkunde, Oberursel, 1987) p. 231.
20. K. H. KLOOS and B. KAISER, in Proceedings of the Conference on Residual Stresses – Measurement, Calculation, Evaluation, Darmstadt, April 1990, edited by V. Hauk, H. Hougardy and E. Macherauch, (Deutsche Gesellschaft für Metallkunde, Oberursel, 1991) p. 205.
21. B. EIGENMANN and E. MACHERAUCH, *Mat.-wiss. u. Werkstofftech.* **26** (1995) 148.
22. *Idem. ibid* **26** (1995) 199.
23. *Idem*, *ibid* **27** (1996) 426.
24. A. PEITER "Residual Stresses of the 1st Kind – Determination and Assessment," (Michael Triltsch Verlag, Düsseldorf, 1966), (in German).
25. E. MACHERAUCH and K. H. KLOOS, in Proceedings of the International Conference on Residual Stresses, Vol. 1, Garmisch Partenkirchen (FRG), 1986, edited by E. Macherauch and V. Hauk, (Deutsche Gesellschaft für Metallkunde, Oberursel, 1987) p. 3.
26. E. HOUDREMONT and H. SCHOLL, *Techn. Mitt. Krupp* **17** (1959) 153, (in German).
27. P. S. PREVEY, in "Materials Characterization," Vol. 10 edited by R.E. Whan (ASM International, Materials Park, OH, 1992) p. 380.
28. D. G. GROSSMAN, *J. Amer. Ceram. Soc.* **55** (1972) 446.
29. G. VIEREGGE "Machining of Iron Materials," (Verlag Stahleisen, Düsseldorf, 1970), (in German).
30. G. B. GREENOUGH, *J. Iron Steel Inst.* **169** (1951) 122.
31. E. MACHERAUCH and P. MÜLLER, *Z. Angew. Physik* **13** (1961) 305, (in German).
32. V. M. HAUK and E. MACHERAUCH, "Advances in X-ray Analysis," edited by J. B. Cohen, J. C. Russ, D. E. Leyden, C. S. Barrett and P. K. Predecki, (1984) p. 81.
33. J. DOMES, PhD thesis, University Erlangen-Nürnberg, Erlangen, (1995), (in German).
34. B. EIGENMANN, W. WÜST, B. SCHOLTES and E. MACHERAUCH, in Proceedings of the International Conference on Residual Stresses, Vol. 1, Garmisch Partenkirchen (FRG), 1986 edited by E. Macherauch and V. Hauk (Deutsche Gesellschaft für Metallkunde, Oberursel, 1987) p. 233.
35. H. SEIBT, PhD Thesis, Universität Hannover, VDI-Verlag, Düsseldorf (1993), (in German).
36. T. LEVERENZ and B. EIGENMANN, Non-destructive Measurement of gradient-type Residual Stress States in machined Ceramic Surfaces (in German), IKM Report, 1994.
37. D. AMOS, B. EIGENMANN and E. MACHERAUCH, *Z. Metallkde* **85** (1994) 317.
38. B. EIGENMANN, B. SCHOLTES and E. MACHERAUCH, *Mat.-wiss. u. Werkstofftech.* **20** (1989) 314.
39. *Idem*, *ibid* **20** (1989) 356.
40. S. IWANAGA, H. NAMIKAWA and S. AOYAMA, *J. Soc. Mater. Sci. Jpn.* **21** (1972) 1106.
41. C. DIERKEN, F. GRELLNER, P. GREIL, J. SINDEL and A. PETSCHELT, in "Bioceramics – Materials and Applications," Vol. 2, edited by R. P. Rusin and G. S. Fischman, (The American Ceramic Society, Westerville, OH, 1995) p. 129.

42. J. SINDEL, F. GRELLNER, C. DIERKEN, P. GREIL and A. PETSCHELT, *J. Mater. Sci. Mater. Med*., (in press).
43. D. G. GROSSMAN, in Proceedings of the International Symposium on Computer Restorations, Regensdorf-Zuerich, May 1991, edited by W. H. Moermann (Quintessenz Publishing Company, Berlin, 1992) p. 103.
44. L. R. PINCKNEY, in "Ceramics and Glasses," (ASM International, Materials Park, OH, 1991) p. 433.
45. J. R. KELLY, H. LUETHY, A. GOUGOULAKIS, P. L. POBER and W. H. MOERMANN, in Proceedings of the International Symposium on Computer Restorations, Regensdorf-Zurich, May 1991, edited by W. H. Moermann (Quintessenz Publishing Company, Berlin, 1992) p. 253.
46. H. K. XU and S. JAHANMIR, *J. Amer. Ceram. Soc*. **78** (1995) 497.
47. T. K. KELLY, *Trans. Inst. Min. Metall*. **75** (1966) 59.
48. K. LONSDALE (ed.) International Tables of X-ray Crystallography, Vol. **3** (Kynoch, Birmingham 1968).
49. L. PINTSCHOVIUS, E. MACHERAUCH and B. SCHOLTES, in Proceedings of the International Conference on Residual Stresses, Vol. 1, Garmisch Partenkirchen (FRG), 1986, edited by E. Macherauch and V. Hauk (Deutsche Gesellschaft für Metallkunde, Oberursel, 1987) p. 159.
50. B. D. CULLITY, "Elements of X-ray Diffraction," (Addison Wesley, Reading, MA, 1978).

Received 17 October 1996
and accepted 1 May 1997